(12) INTERNATIONAL APPLICATION PUBLISHED UNDER THE PATENT COOPERATION TREATY (PCT)

(19) World Intellectual Property Organization
International Bureau

(43) International Publication Date
27 September 2007 (27.09.2007)

PCT

(10) International Publication Number
WO 2007/108980 A1

(51) International Patent Classification:
C04B 35/26 (2006.01) *C04B 35/32* (2006.01)
C04B 35/28 (2006.01) *C04B 35/36* (2006.01)

(21) International Application Number:
PCT/US2007/006164

(22) International Filing Date: 12 March 2007 (12.03.2007)

(25) Filing Language: English

(26) Publication Language: English

(30) Priority Data:
60/781,859 13 March 2006 (13.03.2006) US
60/781,813 13 March 2006 (13.03.2006) US

(71) Applicant *(for all designated States except US)*: **NDSU RESEARCH FOUNDATION** [US/US]; 1735 NDSU Research Foundation, P.O. Box 5002, Fargo, ND 58105 (US).

(72) Inventors; and

(75) Inventors/Applicants *(for US only)*: **SCHULZ, Douglas, Lloyd** [US/US]; 3027 Lakeshore Drive, Moorhead, Minnesota 56560 (US). **SAILER, Robert, A.** [US/US]; 3924 12th Street West, West Fargo, North Dakota 58078 (US). **CARUSO, Anthony, Nicholas** [US/US]; 328 Liberty Lane, Horace, North Dakota 58047 (US).

(74) Agent: **CARTER, Charles, G.**; Foley & Lardner, LLP, 777 E. Wisconsin Avenue, Milwaukee, WI 53202 (US).

(81) Designated States *(unless otherwise indicated, for every kind of national protection available)*: AE, AG, AL, AM, AT, AU, AZ, BA, BB, BG, BR, BW, BY, BZ, CA, CH, CN, CO, CR, CU, CZ, DE, DK, DM, DZ, EC, EE, EG, ES, FI, GB, GD, GE, GH, GM, GT, HN, HR, HU, ID, IL, IN, IS, JP, KE, KG, KM, KN, KP, KR, KZ, LA, LC, LK, LR, LS, LT, LU, LY, MA, MD, MG, MK, MN, MW, MX, MY, MZ, NA, NG, NI, NO, NZ, OM, PG, PH, PL, PT, RO, RS, RU, SC, SD, SE, SG, SK, SL, SM, SV, SY, TJ, TM, TN, TR, TT, TZ, UA, UG, US, UZ, VC, VN, ZA, ZM, ZW.

(84) Designated States *(unless otherwise indicated, for every kind of regional protection available)*: ARIPO (BW, GH, GM, KE, LS, MW, MZ, NA, SD, SL, SZ, TZ, UG, ZM, ZW), Eurasian (AM, AZ, BY, KG, KZ, MD, RU, TJ, TM), European (AT, BE, BG, CH, CY, CZ, DE, DK, EE, ES, FI, FR, GB, GR, HU, IE, IS, IT, LT, LU, LV, MC, MT, NL, PL, PT, RO, SE, SI, SK, TR), OAPI (BF, BJ, CF, CG, CI, CM, GA, GN, GQ, GW, ML, MR, NE, SN, TD, TG).

Published:
— *with international search report*
— *before the expiration of the time limit for amending the claims and to be republished in the event of receipt of amendments*

[Continued on next page]

(54) **Title:** SUPERPARAMAGNETIC COBALT IRON OXYGEN NANOPARTICLES

(57) **Abstract:** Thermal treatment of transition metal ferrite nanoparticles at moderate temperatures (e.g., 500°C to 8500C) provides materials with unanticipated magnetic properties. AxFe3. xθ4-y nanoparticles, e.g., with metal ratio from x = 0.4 to 1.0, can be prepared according to standard solution micelle syntheses. While the as-synthesized materials, such as CoFe2O4 nanoparticles, appeared to be comprised of mainly the magnetite phase (e.g., CoFe2O4) by x-ray diffraction, multiphase materials (e.g., α-Fe and/or zero valent CoFe + CoFe2O4) were observed after the transition metal ferrite nanoparticles were subjected to thermal treatment under nitrogen. Magnetization as a function of applied field and temperature reveal variations in saturation magnetization, coercivity, blocking temperature and Verwey transition temperature dependence as a function of composition. Extremely high saturation magnetization (180 emu/g) with low coercivity (30 Oe or lower) can be achieved with such compositions, which drastically deviates from bulk values of the phases which make up the material and may be attributed to the reduced surface spin disorder and low anisotropy energy induced as a function of the fabrication procedure.

WO 2007/108980 A1

SUPERPARAMAGNETIC COBALT IRON OXYGEN NANOPARTICLES

Government Rights Statement

The U.S. Government has a paid-up license in this invention and the certain other right in the invention as a result of support for this work for by Defense Microelectronics Activity (DMEA) under agreement DMEA 90-02-2-0218 and the National Science Foundation through ND EPSCoR grant EPS-0447679.

Cross Reference to Related Applications

This application claims priority under 35 U.S.C. § 119(e) of U.S. Provisional Application Serial Nos. 60/781,813, 60/781,859 both of which were filed on March 13, 2006, the disclosures of which are herein incorporated by reference in their entireties.

INTRODUCTION

Superparamagnetic (SPM) nanoparticles are multifunctional materials where size provides utility for both magnetic exchange and use.. The overwhelming application interest provides strong impetus toward understanding and controlling the phase, composition and size as relates to the basic magnetic response. Transition metal oxide nanoparticles are simple and inexpensive to fabricate in large quantities with uniform physical and magnetic properties and can be encapsulated, functionalized or left naked as an ambient stable oxide.

Many basic studies of transition metal oxide nanoparticles have been completed that relate magnetic response – coercivity (H_c), saturation magnetization (M_s), relaxation time, permeability and/or blocking (T_B), Verwey (T_V) or Curie (T_C) transition – to raw diameter, shape or crystalline anisotropy, composition, coordination, density, exchange interaction, phase or structure, surface effects, spin-orbit coupling and/or system temperature. Such studies have provided many gross trends: (1) decreasing particle size leads to decreased H_c

and T_c; (2) surface spin disorder leads to surface anisotropy with increased H_c; (3) greater spin-orbit coupling leads to increased exchange anisotropy that tends to increase H_c. For cobalt ferrites specifically, the canonical role of cobalt has been to increase H_c due to an increased anisotropy. A series of compositions and phases of nanoparticles containing chromium, manganese, iron, cobalt, and/or nickel with iron and oxygen with magnetic responses over a threshold that do not fit with present models for M_s and/or H_c (relative to canonical transition metal oxides) are described herein.

SUMMARY

One embodiment relates to superparamagnetic transition metal, iron and oxygen nanoparticles having a saturation magnetization of at least about 100 emu/g, wherein the transition metal may comprise chromium, manganese, iron, cobalt, and/or nickel.

Another embodiment relates to transition metal iron oxygen nanoparticles formed by a process which comprises: a) forming $\bar{A}_xFe_{3-x}O_4$ particles via micellular synthesis; and b) heating the $\bar{A}_xFe_{3-x}O_4$ particles in an oven at about 450°C to 850°C. $\bar{A}$ may be selected from the group consisting of chromium, manganese, cobalt, and/or nickel.

Yet another embodiment relates to superparamagnetic transition metal, iron and oxygen nanoparticles having a saturation magnetization of at least about 80 emu/g and a coercivity (H_c) of no more than about 75 Oe.

FIGURE CAPTIONS

Figure 1.

X-ray diffraction results for the particles **6N5**, **6N8**, **6O5** and **6O8**. The markers at the bottom of the figure indicate individual phases; ▲ spinel ferrite Fe_3O_4, $CoFe_2O_3$ or Fe_2O_3; ▼ Wairauite CoFe; ■ non-spinel Hematite Fe_2O_3; and ◆ iron α-Fe.

Figure 2.

Magnetization as a function of applied field on the particle system **6N5**. The black solid line is for measurements completed at 300 K, while the red dashed curve was completed at 5 K. The inset demonstrates the low coercive and remnant values despite anisotropy inducing cobalt.

Figure 3.

Field cooled and non-field cooled magnetization as a function of temperature on the particle systems **6N5** and **6N7** with the Verwey and blocking temperature identified.

Figure 4a.

FWHM of the 35.4° peak used for Scherrer analysis of the **6N5** treated particles.

Figure 4b.

TEM image of the as synthesized Co0.6Fe2.4O4 particles demonstrating the spherical shape and uniformity.

EXPERIMENT

$Co_xFe_{3-x}O_4$ nanoparticles with x = 0.6, 0.8 and 1.0 were prepared according to a micelle approach previously reported by Li et al., *J. Alloys. Compounds*, **349**, 264 (2003), the disclosure of which is herein incorporated by reference. In brief, targeted amounts of high purity (i.e., 99.998+%) iron nitrate hydrate and cobalt nitrate hydrate were dissolved in 18 MΩ deionized to give an total metals molarity of between 0.01 and 0.02 mol/L. To this solution was added sodium dodecylsulfate (SDS) to give a concentration of between 0.03 and 0/06 mol/L. The mixture was then heated to 50°C in a water bath. A 6M NaOH solution was warmed to 50°C and 0.045 mol of this stock solution was added to the reaction mixture yielding a brownish-yellow precipitate. After cooling, the reaction solvent was decanted and the SDS was extracted from the residual cobalt ferrite nanoparticles with acetone in a Soxhlet extractor. These materials were dried in an oven over night at 80°C and stored in a sealed vial until being subjected to the thermal treatments.

For the thermal treatments, approximately 50 mg aliquots of the $Co_xFe_{3-x}O_4$ particles were loaded into alumina crucibles and placed onto a quartz boat and then moved into the center of a three-zone quartz tube Linberg furnace. After the end cap was put into place, the tube was purged with reactant gas (i.e., nitrogen or oxygen) until 10X the volume of the tube had passed over the samples and through the exit oil bubbler. After the flow rate was reduced to a trickle, the samples were subjected to thermal treatment at either 500°C, 600°C, 700°C or 800°C with total time of ~2 hours at maximum temperature followed by a slow cool to ambient temperature. This cooling rate was controlled and for higher temperatures the oven was allowed to cool overnight. For simple naming, the thermal treated particles are herein be referred to by the designation " xGT", where x is the cobalt stoichiometry (e.g., x=6 refers to $Co_{0.6}Fe_{3.4}O_4$, x=10 refers to $CoFe_3O_4$), G the background gas during reduction (N –nitrogen; O – oxygen) and T the temperature during thermal treatment (X 100 °C) so "**6N5**" refers to $Co_{0.6}Fe_{2.4}O_4$ annealed in nitrogen at 500°C.

Magnetization as a function of temperature (5-400K) and applied field (0-9T) were completed using a Quantum Design physical properties measurement system (PPMS) with the vibrating sample magnetometer (VSM) option, calibrated by a DyO standard. The superconducting magnets were zeroed before each non-field cooled measurement and the VSM frequency was held at 40 Hz. X-ray diffraction (XRD) measurements were performed with a Brukker X-8 diffractometer using Cu Kα for the 2θ range 15-70° with the samples mounted on glass by slurry deposition. The instrumental line broadening was calibrated for use in Scherrer analysis to determine particle diameters. Diluted samples were placed on 300 mesh Formvar coated grids using an eppendorf micropipette and immediately wicked off with filter paper. After allowing the sample to dry, images were obtained using a JEOL 100CX II Transmission Electron Microscope at 100,000X magnification and 80 KeV.

RESULTS

Structure and Phase

The XRD results for cobalt lean compositions **6N5**, **6N8**, **6O5** and **6O8** are shown in Figure 1. The canonical indexes at 2θ=30.1, 35.5, 43.0, 53.5, 57.0 and 62.5° for the spinel ferrites Fe_3O_4, $CoFe_2O_4$ and Fe_2O_3 are observed weakly for all compositions measured. In the case of **6O5**, the particles possess less crystalline phase than all others recorded and a small peak at 20.5° could indicate a trace presence of CoO. For the **6O8** particles, a mixture of the spinel based magnetite and non-spinel based Fe_2O_3 hematite is indicated. The **6N5** particle spectra reveals the presence of a CoFe (Wairauite) phase at 44.9°, that is unique from α-Fe, amongst the spinel ferrite. Lastly, the **6N8** particle composition demonstrates a sharp peak at 44.7° indicating the presence of α-Fe. The intensity and linewidth of this α-Fe strangely suggest the presence of large iron grains, in excess of 100 nm, which does not appear to be the case based on the totality of information available from characterizing the **6N8** particle composition.

Magnetic Measurements

Magnetization as a function of applied field was completed for all composition and treatment parameters, where the values of H_c, M_s and M_r are compiled in Table 1. The coercivity values range from 4 to 1199 Oe, with remnant magnetization results from 0.03 to 28.7 emu/g, while the saturation values pan an astonishing range from 20 to 159 emu/g. An example curve, to demonstrate the shape of magnetization onset for all of the particles is given by Figure 2. Magnetization as a function of temperature was completed by both field cooled (FC) and non-field cooled (NFC) to help determine the blocking and Verwey transition points. Figure 3 shows the M(T) results for the **8N5**, **8N8**, **8O5** and **8O8** particles, where the field applied during cooling was 2 T.

Particle Diameter

The diameter of each treated nanoparticle has been calculated (d_{max}) and is compiled in Table 1 as determined by Equation 1, following use of the Langevin function [^], where k is the Boltzmann constant, T is temperature, (dM/dH) is the slope of the initial (virgin) magnetization curve, ρ is the density and M_s is the saturation magnetization. Equation 1

$$d_{\max} = \left[\frac{18kT(dM/dH)_{H=0}}{\pi \rho M_s^2} \right]^{1/3} \qquad (1)$$

in essence, determines the least upper bound of particle size from the largest magnetization contribution as the initial field is applied; such an analysis may also allow a further determination as to whether small crystallites are buried within other material. Particle diameters were also determined by TEM and through XRD by Scherrer analysis [%]. The comparison between all three methods, using the TEM determination as the standard, yielded dissimilar values. The magnetization calculation (Eqn. 1) underestimated particle size compared to Scherrer analysis which overestimated the diameters. Although it is beyond the scope of this paper to examine why these three methods differ by more than 15 nm, it is noteworthy to ask what can be learned about the physical or magnetic structure of the nanoparticles relative to the assumptions used in the model to generate the diameters. That is, following Langevin theory, we know that when M varies linearly with H, a proportionality can be made to the number of atoms making up each particle; however, as the number of particles is reduced to the superparamagnetic limit, the thermal energy barrier is reduced and the ability to saturate at low fields increases whereby the Langevin constant may exceed 1/3. Hence, smaller than actual diameters calculated from Langevin theory may be crudely used to indicate the presence of superparamagnetic behavior.

DISCUSSION

Treatment and Composition Dependence on Nanoparticle Magnetic Response

Many trends in magnetic response with respect to nanoparticle preparation conditions can be extracted from Table 1 and correlated with findings from XRD and particle diameter calculations. One of the most noticeable trends is the tremendous increase in coercivity of all three compositions treated in oxygen at 800 C relative to all other treated particles. We attribute these high H_c values to a high uniaxial anisotropy in the standard $CoFe_2O_4$ spinel phase and these particles are larger overall; however, the coercivity does not significantly decrease with decreased cobalt content as found by others . For all the particles treated in oxygen and those treated in nitrogen at 800 C, a reduced saturation magnetization relative to bulk $CoFe_2O_4$ is found. This reduction in M_s follows arguments regarding surface spin disorder and resulting anisotropy. With respect to results published by Betancourt et al., who found that increased cobalt content leads to significantly decreased M_s, we again find conflicting results where saturation magnetization is very consistent between compositions and only different by treatment conditions.

In the case of all compositions treated in nitrogen at 600 C or above, a tremendously high M_s value is found relative to all other cobalt ferrite nanoparticle reports and to bulk cobalt ferrite (90 emu/g). Because the saturation values are so high (159 emu/g) relative to bulk cobalt ferrite an explanation involving other phases or exotic mechanisms must occur. Without knowing the exact ionic distribution or degree of inversion of the spinel structure and will be explored in the next section.

Treatment Implications on Nanoparticle Structure

The XRD results for the **6N5**, **6N8**, **6O5** and **6O8** compositions indicate a mixture of phases that makeup the nanoparticles. An illustration of the real space nanoparticle makeup may not be drawn soley from the qualitative XRD results, but may be constructed by combining such results with the magnetic measurements and some knowledge of transition metal reduction. It should be noted that above 595 C, the cobalt ferrite particles reduce, similar to Fe_3O_4 reduction to α-Fe observed by others and ascribed to the Hedval mechanism. For the **6N8** nanoparticle system, the XRD results indicate a large presence of α-Fe with some accompanying spinel based ferrite phase. The magnetic measurements on **6N8** indicate an H_c=31 Oe, M_r= 0.9 emu/g, and M_s=159 emu/g. Because of the presence of iron, the small coercivity and the large remnant magnetization, one possible model is that of iron nanoparticles embedded in cobalt ferrite, where the iron particle size is close to or below the superparamagnetic limit.

Temperature Dependence of the Magnetization

Magnetization as a function of temperature for the **6N5** and **6N8** treated particles as seen in Figure 3 indicate two transitions in both the FC and NFC measurements. The first intensity reduction at 120 K may be attributed to the Verwey transition as observed by others, with the higher temperature transition indicating the blocking temperature. For the **6N5**, which we believe is composed of cobalt ferrite and trace CoFe, the value of T_B is on average with other reports.

CONCLUSION

A diverse range of magnetic responses have been obtained from a set of cobalt variable ferrite compositions and treatment conditions. The treatment conditions yield multiple phase nanoparticles with both stoichiometric and non-stoichiometric compositions that are phase separated; such a determination has been made through combined x-ray diffraction and magnetization measurements. Of special interest are all those particles treated in nitrogen at or above 600°C, which demonstrate Ms values greater than and Hc values less than bulk cobalt ferrite. The model generated for this system is nanocrystals of iron, whose diameter is at or below the superparamagnetic limit, embedded in a ferrite matrix, with ferrite or oxide residing at the surface. The special emphasis of these particles are due to their application interest wherein refractory superparamagnetic particles with extreme saturation moments and low coercivity, relative to other ferrite nanoparticles, may be produced in large quantities and inexpensively.

Illustrative Embodiments

The present superparamagnetic transition metal iron oxygen nanoparticles and related methods of producing such particles and/or using such are further exemplified by the following claims and descriptions, which are not intended to limit the scope of the invention disclosed herein.

1. Superparamagnetic transition metal iron oxygen nanoparticles having a saturation magnetization of at least about 100 emu/g {in some instances $\geq$ 125 emu/g and, in others $\geq$ 150 emu/g}; wherein the nanoparticles typically include zero valent metal clusters, e.g., ., α-Fe and/or transition metal/Fe alloy.

The nanoparticles of embodiment 1 wherein said nanoparticles have a coercivity (H_c) of no more than about 75 Oe. {in some instances $\leq$ 50 Oe and, in others $\leq$ 35 Oe}

The nanoparticles of embodiment 1 comprising $Co_xFe_{3-x}O_4$ particles; wherein x has a value of 0.4 to 1.0.

Superparamagnetic transition metal ferrite nanoparticles having a saturation magnetization of at least about 100 emu/g.

Superparamagnetic transition metal iron oxygen nanoparticles having a saturation magnetization of at least about 100 emu/g and a coercivity (H_c) of no more than about 75 Oe.

Superparamagnetic transition metal iron oxygen nanoparticles having a saturation magnetization of at least about 50 emu/g and a coercivity (H_c) of no more than about 10 Oe.

Superparamagnetic transition metal iron oxygen nanoparticles having a saturation magnetization of at least about 125 emu/g and a coercivity (H_c) of no more than about 35 Oe.

Superparamagnetic transition metal iron oxygen nanoparticles having a saturation magnetization of at least about 150 emu/g and a coercivity (H_c) of no more than about 50 Oe.

Superparamagnetic transition metal iron oxygen nanoparticles having a saturation magnetization of at least about 150 emu/g and a coercivity (H_c) of no more than about 75 Oe.

Superparamagnetic transition metal iron oxygen nanoparticles having a saturation magnetization of at least about 20 emu/g and a coercivity (H_c) of no more than about 5 Oe.

Superparamagnetic transition metal iron oxygen nanoparticles having a saturation magnetization of at least about 150 emu/g; a remnant magnetization of no more than about 5 emu/g; and a coercivity (H_c) of no more than about 35 Oe.

Superparamagnetic transition metal iron oxygen nanoparticles having a saturation magnetization of at least about 50 emu/g and a coercivity (H_c) of no more than about 20 Oe.

Superparamagnetic transition metal iron oxygen nanoparticles having a saturation magnetization of at least about 150 emu/g; and a remnant magnetization of no more than about 5 emu/g.

Superparamagnetic transition metal iron oxygen nanoparticles having a saturation magnetization of at least about 100 emu/g; and a remnant magnetization of no more than about 10 emu/g;

Superparamagnetic transition metal iron oxygen nanoparticles having a saturation magnetization of at least about 15 emu/g; and a remnant magnetization of no more than about 0.5 emu/g.

Superparamagnetic transition metal iron oxygen nanoparticles having a saturation magnetization of at least about 20 emu/g; and a remnant magnetization of no more than about 0.1 emu/g;

Superparamagnetic transition metal iron oxygen nanoparticles having a saturation magnetization of at least about 125 emu/g; and a remnant magnetization of no more than about 5 emu/g.

Superparamagnetic transition metal iron oxygen nanoparticles having a saturation magnetization of at least about 50 emu/g; and a remnant magnetization of no more than about 2 emu/g;

25. Transition metal iron oxygen nanoparticles formed by a process which comprises:

a) forming $A_xFe_{3-x}O_4$ particles via micellular synthesis;

b) heating the $A_xFe_{3-x}O_4$ particles at about 450°C to 850 °C.

wherein A is a transition metal selected from the group consisting of cobalt, manganese, chromium, and/or nickel.

The nanoparticles of embodiment 25 wherein x has a value of 0.4 to 1.0.

The nanoparticles of embodiment 25 wherein said nanoparticles are superparamagnetic.

The nanoparticles of embodiment 25 wherein the forming operation includes precipitating particles from an aqueous solution which includes iron nitrate hydrate, transition metal nitrate hydrate and sodium dodecylsulfate (SDS).

The nanoparticles of embodiment 25 wherein the heating operation includes heating the

$Co_xFe_{3-x}O_4$ particles at about 550°C to 850°C.

The nanoparticles of embodiment 25 wherein the heating operation includes heating the

$Co_xFe_{3-x}O_4$ particles for about 1 to 10 hours.

The nanoparticles of embodiment 25 wherein the heating operation includes heating the

$Co_xFe_{3-x}O_4$ particles under a nitrogen atmosphere.

The nanoparticles of embodiment 25 wherein x has a value of at least about 0.7.

The nanoparticles of embodiment 25 wherein the heating operation includes heating the

$Co_xFe_{3-x}O_4$ particles at about 750°C to 850°C.

The nanoparticles of embodiment 25 wherein the heating operation includes heating the

$Co_xFe_{3-x}O_4$ particles in an oven at about 550°C to 850°C under a nitrogen atmosphere.

Superparamagnetic transition metal iron oxygen nanoparticles having a saturation magnetization of at least about 125 emu/g and a coercivity (H_c) of no more than about 50 Oe.

Such superparamagnetic transition metal iron oxygen nanoparticles having a saturation magnetization of at least about 100 emu/g; a remnant magnetization of no more than about 5 emu/g; and a coercivity (H_c) of no more than about 50 Oe.

The nanoparticles of embodiment 25 wherein the heating operation includes heating the

$A_xFe_{3-x}O_4$ particles at about 450°C to 550°C.

Superparamagnetic transition metal iron oxygen nanoparticles having a saturation magnetization of at least about 50 emu/g and a coercivity (H_c) of no more than about 20 Oe.

Such superparamagnetic transition metal iron oxygen nanoparticles having a saturation magnetization of at least about 50 emu/g; and a remnant magnetization of no more than about 2 emu/g.

The nanoparticles of embodiment 25 wherein the heating operation includes heating $Co_xFe_{3-x}O_4$ particles under an oxygen atmosphere.

Superparamagnetic transition metal iron oxygen nanoparticles having a saturation magnetization of at least about 20 emu/g and a coercivity (H_c) of no more than about 5 Oe.

Such superparamagnetic transition metal iron oxygen nanoparticles having a saturation magnetization of at least about 15 emu/g; and a remnant magnetization of no more than about 0.1 emu/g.

Such superparamagnetic transition metal iron oxygen nanoparticles having a saturation magnetization of at least about 20 emu/g; a remnant magnetization of no more than about 0.1 emu/g; and a coercivity (H_c) of no more than about 5 Oe.

The nanoparticles of embodiment 25 wherein the heating operation includes heating the

$Co_xFe_{3-x}O_4$ particles at about 450°C to 550°C under an oxygen atmosphere.

The nanoparticles of embodiment 25 wherein said transition metal iron oxygen nanoparticles have an average crystallite diameter of no more than about 100 nm (as determined by TEM).

The nanoparticles of embodiment 25 wherein said transition metal iron oxygen nanoparticles have an average crystallite diameter of no more than about 50 nm (as determined by TEM).

The nanoparticles of embodiment 25 wherein said transition metal iron oxygen nanoparticles have an average crystallite diameter of no more than about 50 nm (as determined by XRD).

The nanoparticles of embodiment 25 wherein said transition metal iron oxygen nanoparticles have an average crystallite diameter of no more than about 50 nm (as determined by TEM).

The nanoparticles of embodiment 25 wherein said transition metal iron oxygen nanoparticles have an average crystallite diameter of no more than about 10 nm (as determined by the Langevin function method).

The nanoparticles of embodiment 25 wherein said transition metal iron oxygen nanoparticles have an average crystallite diameter of no more than about 50 nm (as determined by the Langevin function method).

The nanoparticles of embodiment 25 comprising a spinel phase.

The nanoparticles of embodiment 25 comprising a transition metal ferrite.

The nanoparticles of embodiment 25 having crystallite sizes of about 30 to 75 nm (as determined by powder XRD analysis).

The nanoparticles of embodiment 25 wherein said transition metal iron oxygen nanoparticles have an Mr/Ms ratio of no more than about 0.1.

The nanoparticles of embodiment 25 wherein said transition metal iron oxygen nanoparticles have an Mr/Ms ratio of no more than about 0.01.

The nanoparticles of embodiment 25 comprising $Co_xFe_{3-x}O_4$ particles; wherein x has a value of 0.4 to 1.0.

The nanoparticles of embodiment 25, wherein said nanoparticles include transition metal ferrite nanoparticles.

X. An inorganic/polymer composite material comprising any of the superparamagnetic transition metal iron oxygen nanoparticles described above.

The inorganic/polymer composite material of embodiment X further comprising a thermoplastic polymer.

The inorganic/polymer composite material of embodiment X further comprising a thermoplastic elastomer.

Y. A flexible coating material comprising the inorganic/polymer composite material of embodiment X.

Q. A composite material comprising any of the superparamagnetic transition metal iron oxygen nanoparticles described above.

The composite material of embodiment Q further comprising a ceramic matrix having the nanoparticles embedded therein.

Z. A process of forming transition metal iron oxygen nanoparticles which comprises:

a) forming $A_xFe_{3-x}O_4$ particles via micellular synthesis;

b) heating $A_xFe_{3-x}O_4$ particles in an oven at about 450°C to 850°C;

wherein A is selected from the group consisting of cobalt, manganese, chromium, nickel, iron and mixtures thereof.

Za. The process of embodiment Z wherein the forming operation includes precipitating particles from an aqueous solution formed from a mixture of ingredients which includes iron nitrate hydrate, transition metal nitrate hydrate and sodium dodecylsulfate.

The process of embodiment Za further comprising drying the precipitated particles prior to the heating operation.

The process of embodiment Z wherein the heating operation includes heating the $Co_xFe_{3-x}O_4$ particles in an oven at about 550°C to 850°C.

The process of embodiment Z wherein the heating operation includes heating the $Co_xFe_{3-x}O_4$ particles for about 1 to 10 hours.

The process of embodiment Z wherein the heating operation includes heating the $Co_xFe_{3-x}O_4$ particles under a nitrogen atmosphere.

The process of embodiment Za wherein the heating operation includes heating the $Co_xFe_{3-x}O_4$ particles in an oven at about 750°C to 850°C.

The process of embodiment Za wherein the heating operation includes heating the $Co_xFe_{3-x}O_4$ particles in an oven at about 595°C or higher.

The process of embodiment Z wherein the heating operation includes heating the $Co_xFe_{3-x}O_4$ particles under an oxygen atmosphere.

The process of embodiment Z wherein the heating operation includes heating the $Co_xFe_{3-x}O_4$ particles at about 450°C to 550°C under an oxygen atmosphere.

Superparamagnetic cobalt iron oxygen nanoparticles having a saturation magnetization of at least about 100 emu/g {in some instances $\geq$ 125 emu/g and, in others $\geq$ 150 emu/g}; wherein the nanoparticles typically include zero valent metal clusters, e.g., ., α-Fe and/or Co/Fe alloy.

Superparamagnetic chromium iron oxygen nanoparticles having a saturation magnetization of at least about 100 emu/g {in some instances $\geq$ 125 emu/g and, in others $\geq$ 150 emu/g}; wherein the nanoparticles typically include zero valent metal clusters, e.g., ., α-Fe and/or Cr/Fe alloy.

Superparamagnetic nickel iron oxygen nanoparticles having a saturation magnetization of at least about 100 emu/g {in some instances $\geq$ 125 emu/g and, in others $\geq$ 150 emu/g}; wherein the nanoparticles typically include zero valent metal clusters, e.g., ., α-Fe and/or Ni/Fe alloy.

Superparamagnetic manganese iron oxygen nanoparticles having a saturation magnetization of at least about 100 emu/g {in some instances $\geq$ 125 emu/g and, in others $\geq$ 150 emu/g}; wherein the nanoparticles typically include zero valent metal clusters, e.g., ., α-Fe and/or Mn/Fe alloy.

Superparamagnetic iron oxygen nanoparticles having a saturation magnetization of at least about 100 emu/g {in some instances $\geq$ 125 emu/g and, in others $\geq$ 150 emu/g}; wherein the nanoparticles typically include zero valent metal clusters, e.g., ., α-Fe.

Superparamagnetic cobalt iron oxygen nanoparticles having a saturation magnetization of at least about 50 emu/g and a coercivity (H_c) of no more than about 10 Oe.

Superparamagnetic chromium iron oxygen nanoparticles having a saturation magnetization of at least about 50 emu/g and a coercivity (H_c) of no more than about 10 Oe.

Superparamagnetic manganese iron oxygen nanoparticles having a saturation magnetization of at least about 50 emu/g and a coercivity (H_c) of no more than about 10 Oe.

Superparamagnetic nickel iron oxygen nanoparticles having a saturation magnetization of at least about 50 emu/g and a coercivity (H_c) of no more than about 10 Oe.

Superparamagnetic iron oxygen nanoparticles having a saturation magnetization of at least about 50 emu/g and a coercivity (H_c) of no more than about 10 Oe.

Transition metal iron oxygen nanoparticles formed by a process which comprises:
a) forming $Co_xFe_{3-x}O_4$ particles via micellular synthesis;
b) heating the $Co_xFe_{3-x}O_4$ particles at about 450°C to 850 °C.

Transition metal iron oxygen nanoparticles formed by a process which comprises:
a) forming $Cr_xFe_{3-x}O_4$ particles via micellular synthesis;
b) heating the $Cr_xFe_{3-x}O_4$ particles at about 450°C to 850 °C.
Transition metal iron oxygen nanoparticles formed by a process which comprises:
a) forming $Mn_xFe_{3-x}O_4$ particles via micellular synthesis;
b) heating the $Mn_xFe_{3-x}O_4$ particles at about 450°C to 850 °C.

Transition metal iron oxygen nanoparticles formed by a process which comprises:
a) forming $Ni_xFe_{3-x}O_4$ particles via micellular synthesis;
b) heating the $Ni_xFe_{3-x}O_4$ particles at about 450°C to 850 °C.

Transition metal iron oxygen nanoparticles formed by a process which comprises:
a) forming Fe_3O_4 particles via micellular synthesis;
b) heating the Fe_3O_4 particles at about 450°C to 850 °C.

Table 1

Values of remnant magnetization (M_r), saturation magnetization (M_s), coercive field (H_c), calculated particle diameter (*d*) and relative permeability (μ) are given as a function for all composition and treatment conditions. d^1 – TEM value, d^2 – Scherrer value, d^3 – Langevin based calculation.

Sample	Ms (emu/g)	Ms (emu/mole)	Hc (Oe)	Relative Permeability	Mr (emu/g)	Mr/Ms	D1 (nm)	D2 (nm)	D3 (nm)
6N5	57	10119.80964	86.1	100.0029	4.29	0.075	16.6	33.8	3.75
6N6	144	25565.83488	147.9	345.173	14.61	0.101	28.8	NA	2.46
6N7	149	26453.53748	76.9	83.35756	5.07	0.034	33.3	64.7	2.2
6N8	159	28228.94268	31.4	120.4594	0.88	0.006	NA	NA	1.72
6O5	20	3550.8104	169.9	9.63756	1.31	0.066	NA	NA	4.29
6O8	31	5503.75612	1198.7	78.57071	13.56	0.437	NA	NA	3.74
8N5	52	9264.22432	33.1	106.5221	1.35	0.026	NA	NA	5.65
8N6	106	18884.76496	32.6	201.6807	5.12	0.048	NA	NA	3.92
8N7	134	23873.19344	129.8	110.8177	4.66	0.035	NA	NA	2.19
8N8	149	26545.56584	57.1	74.65895	3.7	0.025	NA	NA	2.15
8O5	25	4453.954	24.6	278.9748	0.28	0.011	NA	NA	4.2
8O8	72	12827.38752	1082.9	116.0718	28.68	0.398	NA	NA	1.8
10N5	54	9653.8932	14.5	171.7874	1.1	0.02	NA	NA	3.9
10N6	80	14302.064	130.9	73.54557	5.87	0.073	NA	NA	2.49
10N7	120	21453.096	149	311.0598	7.07	0.059	NA	NA	1.94
10N8	132	23598.4056	57.9	332.5066	4.5	0.034	NA	NA	1.97
10O5	20	3575.516	4	28.12625	0.03	0.002	NA	NA	4.31
10O8	27	4826.9466	1198.3	36.65985	11.82	0.438	NA	NA	2.84

We Claim:

1. Superparamagnetic transition metal iron oxygen nanoparticles having a saturation magnetization of at least about 100 emu/g;

wherein the transition metal comprises cobalt, manganese, chromium and/or nickel.

2. The nanoparticles of claim 1 wherein said nanoparticles have a coercivity (H_c) of no more than about 75 Oe.

3. The nanoparticles of claim 1 formed from $A_xFe_{3-x}O_4$ and comprising zero valent metal clusters; wherein x has a value of 0.4 to 1.0 and A is the transition metal.

4. Transition metal iron oxygen nanoparticles formed by a process which comprises:

a) forming $A_xFe_{3-x}O_4$ particles via micellular synthesis;

b) heating the $A_xFe_{3-x}O_4$ particles in an oven at about 450°C to 850°C;

wherein A is selected from the group consisting of cobalt, manganese, chromium, nickel, iron and mixtures thereof.

5. The nanoparticles of claim 4 wherein x has a value of 0.4 to 1.0.

6. The nanoparticles of claim 4 wherein said nanoparticles are superparamagnetic.

7. The nanoparticles of claim 4 wherein the forming operation includes precipitating particles from an aqueous solution which includes iron nitrate hydrate, transition metal nitrate hydrate and sodium dodecylsulfate.

8. The nanoparticles of claim 4 wherein the heating operation includes heating the $A_xFe_{3-x}O_4$ particles in an oven at a temperature of at least about 550°C for at least about one hour.

9. The nanoparticles of claim 4 wherein the heating operation includes heating the $A_xFe_{3-x}O_4$ particles for about 1 to 10 hours.

10. The nanoparticles of claim 4 wherein the heating operation includes heating the $A_xFe_{3-x}O_4$ particles under a nitrogen atmosphere.

11. The nanoparticles of claim 10 wherein x has a value of at least about 0.7.

12. The nanoparticles of claim 10 wherein the heating operation includes heating the $A_xFe_{3-x}O_4$ particles in an oven at a temperature of about 750°C to 850°C.

13. Superparamagnetic transition metal iron oxygen nanoparticles having a saturation magnetization of at least about 50 emu/g and a coercivity (H_c) of no more than about 75 Oe.

14. The nanoparticles of claim 13 wherein the transition metal comprises cobalt, manganese, chromium and/or nickel.

15. The nanoparticles of claim 13 comprising $A_xFe_{3-x}O_4$ particles; wherein x has a value of 0.4 to 1.0 and A is the transition metal.

16. The nanoparticles of claim 13 having a saturation magnetization of at least about 100 emu/g.

17. The nanoparticles of claim 13 having a coercivity (H_c) of no more than about 65 Oe.

18. The nanoparticles of claim 13 having a coercivity (H_c) of no more than about 55 Oe.

19. The nanoparticles of claim 13 having a coercivity (H_c) of no more than about 10 Oe.

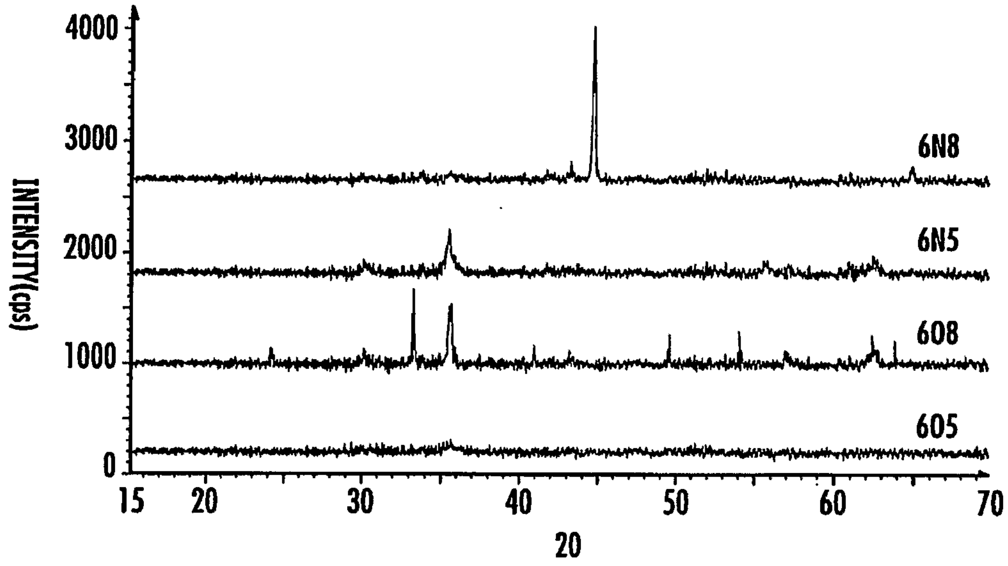
4000
3000
2000
1000
0
INTENSITY(cps)
6N8
6N5
6O8
6O5
15
20
30
40
50
60
70
2θ

FIG. 1

FIG. 2

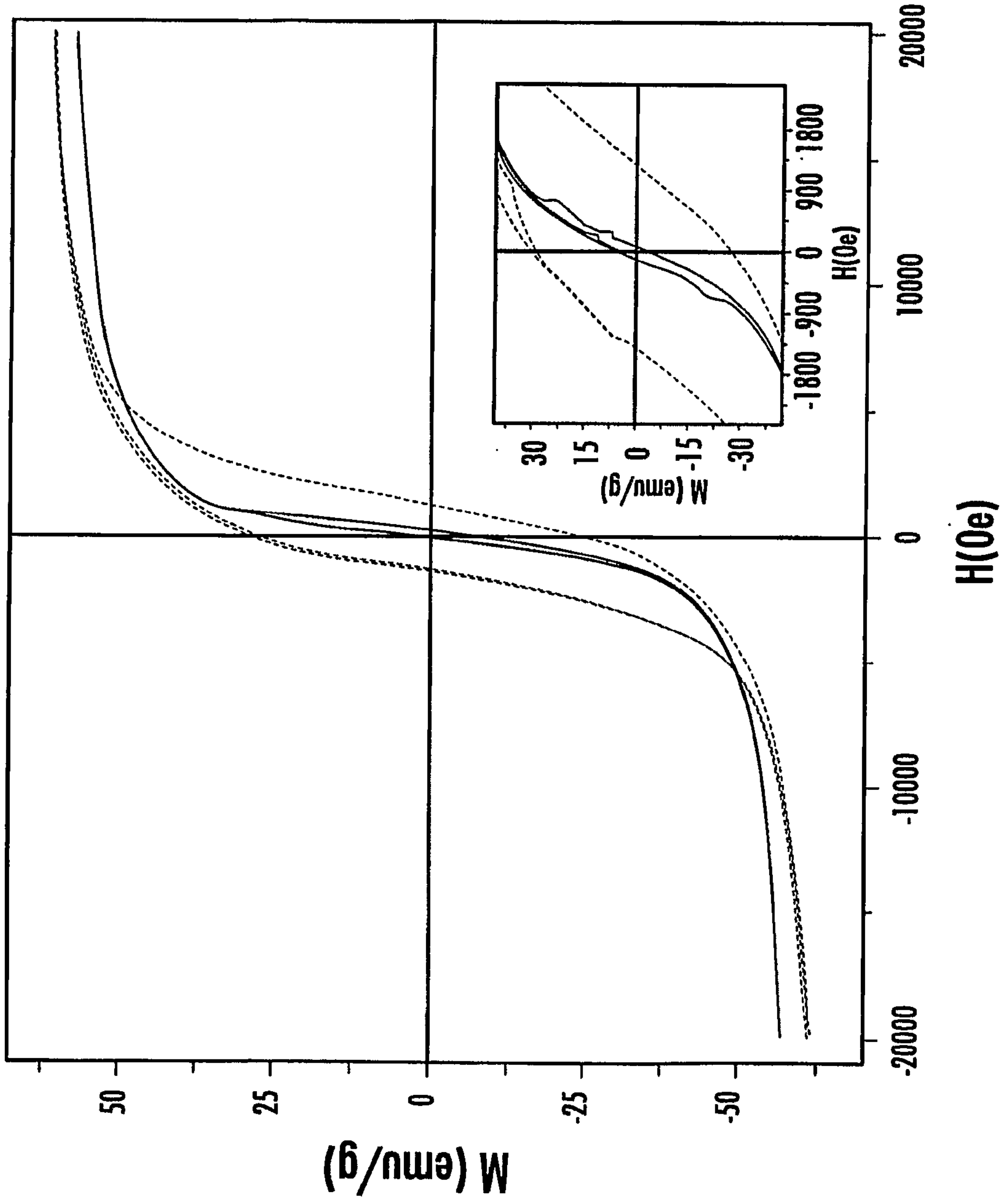
M (emu/g)
50
25
0
-25
-50
H(Oe)
-20000
-10000
0
10000
20000
M (emu/g)
30
15
0
-15
-30
H(Oe)
-1800
-900
0
900
1800

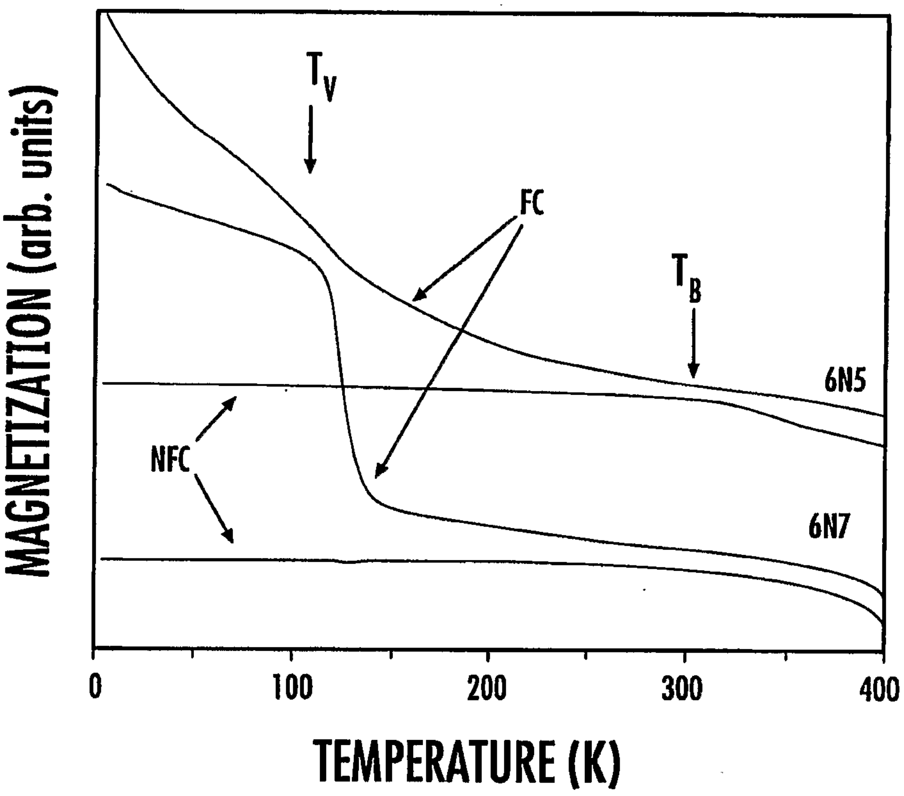
T_V
FC
T_B
6N5
NFC
6N7
0
100
200
300
400
TEMPERATURE (K)
MAGNETIZATION (arb. units)

FIG. 3

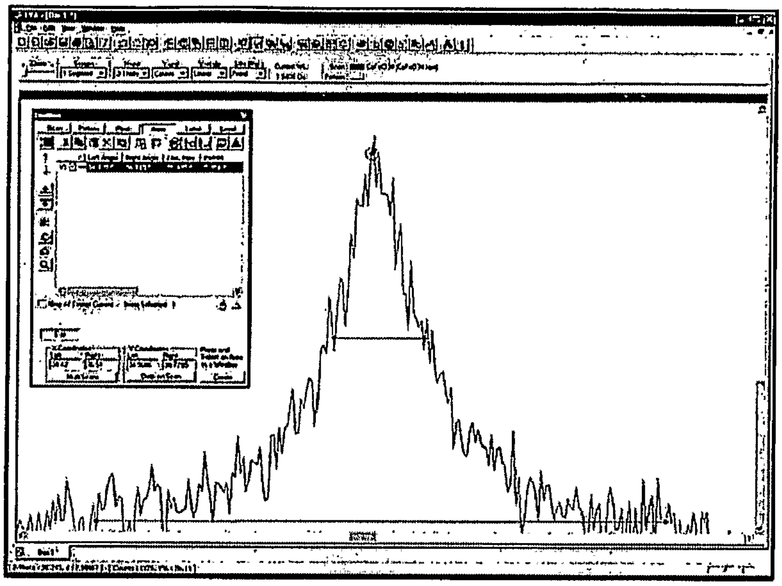

FIG. 4a

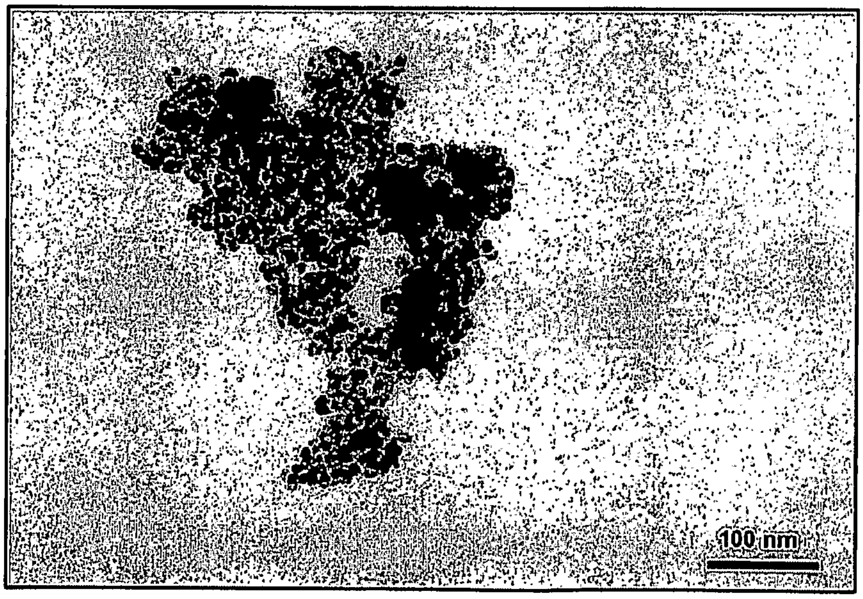

FIG. 4b

INTERNATIONAL SEARCH REPORT

International application No.
PCT/US2007/006164

A. CLASSIFICATION OF SUBJECT MATTER

C04B 35/26(2006.01)i, C04B 35/28(2006.01)i, C04B 35/32(2006.01)i, C04B 35/36(2006.01)i

According to International Patent Classification (IPC) or to both national classification and IPC

B. FIELDS SEARCHED

Minimum documentation searched (classification system followed by classification symbols)
IPC8 C04B 35/26, 35/28, 35/32, 35/36

Documentation searched other than minimum documentation to the extent that such documents are included in the fields searched
Korean Utility models and applications for Utility models since 1975
Japanese Utility models and applications for Utility models since 1975

Electronic data base consulted during the international search (name of data base and, where practicable, search terms used)
eKIPASS (KIPO internal) " superparamagnetic, nanoparticle, transion metal"

C. DOCUMENTS CONSIDERED TO BE RELEVANT

Category*	Citation of document, with indication, where appropriate, of the relevant passages	Relevant to claim No.
X	US 2004/0253437 A1 (SNORRI THORGEIR INGVARSSON et al.) 16 DECEMBER 2004 see claims 1-14	1-3, 13-19
X	WO 2004/108330 A1 (MICRO TECHNOLOGY CENTRE MANAGEMENT LIMITED) 16 DECEMBER 2004 see the abstract; example; claims	4 - 12
A	US 6262129 B1 (CHRISTOPHER BRUCE MURRAY) 17 JULY 2001 see claims	4
A	US 6797380 B2 (PETER JOHN BONITATEBUS, JR. et al.) 28 SEPTEMBER 2004 see claims 5,7,9,33	1

☐ Further documents are listed in the continuation of Box C.   ☒ See patent family annex.

* Special categories of cited documents:
"A" document defining the general state of the art which is not considered to be of particular relevance
"E" earlier application or patent but published on or after the international filing date
"L" document which may throw doubts on priority claim(s) or which is cited to establish the publication date of citation or other special reason (as specified)
"O" document referring to an oral disclosure, use, exhibition or other means
"P" document published prior to the international filing date but later than the priority date claimed
"T" later document published after the international filing date or priority date and not in conflict with the application but cited to understand the principle or theory underlying the invention
"X" document of particular relevance; the claimed invention cannot be considered novel or cannot be considered to involve an inventive step when the document is taken alone
"Y" document of particular relevance; the claimed invention cannot be considered to involve an inventive step when the document is combined with one or more other such documents,such combination being obvious to a person skilled in the art
"&" document member of the same patent family

Date of the actual completion of the international search 20 AUGUST 2007 (20.08.2007)	Date of mailing of the international search report **21 AUGUST 2007 (21.08.2007)**
Name and mailing address of the ISA/KR Korean Intellectual Property Office 920 Dunsan-dong, Seo-gu, Daejeon 302-701, Republic of Korea Facsimile No. 82-42-472-7140	Authorized officer CHUNG, Jin Sung Telephone No. 82-42-481-8393

INTERNATIONAL SEARCH REPORT

Information on patent family members

International application No.

PCT/US2007/006164

Patent document cited in search report	Publication date	Patent family member(s)	Publication date
US20040253437A1	16.12.2004	US2004188298A1	30.09.2004
		US2004188298AA	30.09.2004
		US2004253437A1	16.12.2004
		US2004253437AA	16.12.2004
W02004108330A1	16.12.2004	AU2004244668AA	16.12.2004
		AU2004244668BB	05.07.2007
		EP1638719A1	29.03.2006
		US2006225535AA	12.10.2006
		US2006225535A1	12.10.2006
US06262129	17.07.2001	AT233938E	15.03.2003
		CN124377A	09.02.2000
		CN1243775	09.02.2000
		CN1328735C	25.07.2007
		DE69905663T2	20.11.2003
		EP00977212A2	02.02.2000
		EP00977212A3	05.07.2000
		EP00977212B1	05.03.2003
		EP0977212A2	02.02.2000
		EP977212A3	05.07.2000
		EP977212B1	05.03.2003
		JP12054012	22.02.2000
		JP2000054012A2	22.02.2000
		JP3258295B2	18.02.2002
		KR1020000011546	25.02.2000
		KR20000011546A	25.02.2000
		SG83738A1	16.10.2001
		US6262129BA	17.07.2001
US06797380	28.09.2004	CN1475459A	. .A
		EP01386886A1	04.02.2004
		EP1386886A1	04.02.2004
		JP16075530	11.03.2004
		JP2004075530A2	11.03.2004
		N020033409A0	30.07.2003
		US2004023030AA	05.02.2004
		US6797380BB	28.09.2004
